

# C-band septum polarizer design

L. Cresci<sup>1</sup>, L. Ciappi<sup>2</sup>, R. Nesti<sup>1</sup>, F. Palagi<sup>3</sup>, D. Panella<sup>1</sup>

<sup>1</sup>INAF-Arcetri Astrophysical Observatory, Largo E. Fermi 5, I-50125 Florence (Italy)

<sup>2</sup>Department of Electronics and Telecommunications-University of Florence,  
Via Lombroso 6/17, I-50134 Florence (Italy)

<sup>3</sup>IRA-CNR Section of Florence, Largo E. Fermi 5, I-50125 Florence (Italy)

**Arcetri Technical Report N° 6/2002**  
**Firenze 2002**

## Abstract

*Low loss dual-polarisation performances are highly required in passive devices for low noise radio astronomy receivers at microwave wavelengths. The use of waveguide polarisers is generally better than optical wire grids especially at very low frequencies when space occupation and weights become predominant factors. In this report, the design and testing of a C-band (6-8 GHz) septum polariser is described. The interest in the development of such a device comes from up-grading demands in receiving instrumentation of the radio telescopes of Noto and Arecibo. The measurements showing very good performances are accurately described and comparison with expected data are presented to show the validity of the design approach.*



techniques adopting the Finite Element Method [3] as implemented in the Ansoft High Frequency Structure Simulator (HFSS v.8) commercial package.

Once high return loss (above 20 dB) for all the four signals (the fundamental TE<sub>10</sub> mode in the two rectangular waveguides and the two orthogonal modes TE<sub>10</sub> and TE<sub>01</sub> in the square waveguide) has been achieved, the design efforts was concentrated to the corrugated region in order to compensate the phase shift and to have a circular polarisation excitation as pure as possible. To this purpose, proprietary codes [4] based on the Mode Matching technique [5] have been used.

As these two problems have been solved, interface problems were faced on. In particular a suitable double stepped transition has been design to have the input ports in standard WR137 and a square to circular transition has been studied as the output must be connected to a corrugated circular horn.

Finally the structure shown in Fig. 1 results with an overall length of about 30cm.

At present the device is optimised in the 6.3 - 7.1 GHz frequency band. The electromagnetic performances are given later on.

The reflection coefficients of the two orthogonal linear polarised fields at the common output port are shown in Fig. 2. These data may be combined to obtained the return loss of the two circular polarisations at the same port.

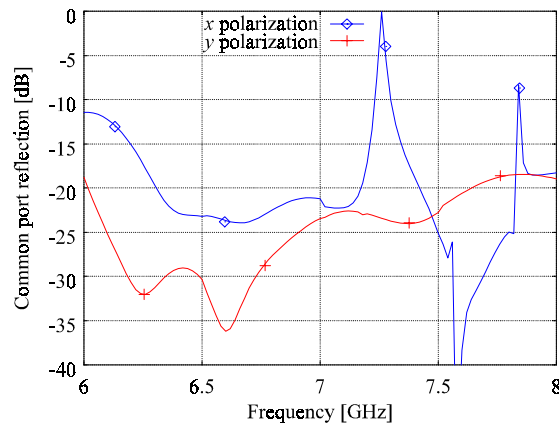


**Fig. 2:** Common port scattering parameters.

Two undesired resonances show up at 7.25 GHz and 7.8 GHz. A lot of work was done to try to remove them without success. Our conclusion is that it could be possible to shift the resonant frequencies by changing the geometry of the polariser, but impossible to remove them, as they are somehow connected to the electromagnetic behaviour of this kind of structure.

This is particularly true for the first resonance. The second one, at the higher frequency, is associated with the square to circular transition and it is possible to work on it to cancel this effect. However, in this higher frequency band, higher order modes are excited in the polariser (for example the cut-off frequency of the TE<sub>11</sub> mode in the square waveguide is about 7.47 GHz), so it is more difficult to reach an acceptable operation.

A more meaningful characterisation of the polariser is given in Fig. 3.

The two curves show the scattering parameters associated to the input rectangular ports which are more interesting from an operational point of view.

The reflection coefficient at each port, which by symmetry is the same, and the cross talk between them are plotted Vs frequency.

By referring to these parameters and taking -20dB as the upper limit for both of them, the device show dual band operation mode: a broader band between 6.3 and 7.2 GHz and a smaller band between 7.4 and 7.7 GHz. The principal issue is that resonances are very close to the band limits.

Each input rectangular waveguide excites in the common output two 90° polarised signals, one (X) in the x direction and the other (Y) in the y direction. The phase shift (X-Y) between them is plotted in Fig. 4; depending on which port is excited, different values are obtained, but we can say, by symmetry, that the two different excitations produce 180° out-of-phase phase-shift (X-Y). Thus we can use the same graph to represent the two cases and referring each case to different ordinate scale (shifted by 180°). This is done in Fig.4: the left (right) ordinate scale gives the phase shift related to the excitation by the left (right) port.

This performance is a direct measure of the polarisation of the field: if the phase shift  $\Delta\phi$  between the two orthogonal components (x pol.- y pol.) is  $0^\circ < \Delta\phi < 180^\circ$  ( $-180^\circ < \Delta\phi < 0^\circ$ ) then the  $-z$  travelling wave coming out from the common port is left hand (right hand) elliptically polarised. In particular, if the two components are equal in amplitude and the phase shift is  $90^\circ$  ( $-90^\circ$ ) then the polarisation is left hand (right hand) circular.

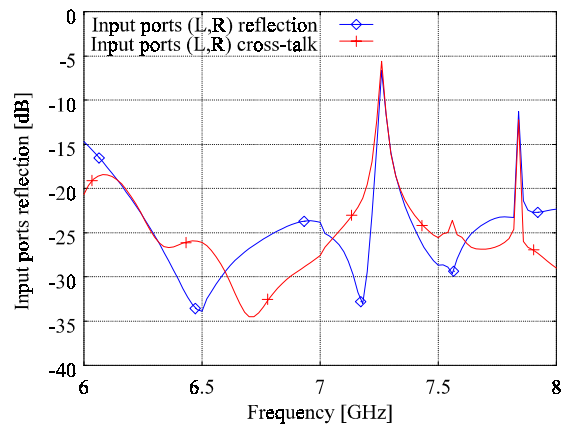


**Fig. 3:** Input rectangular ports scattering parameters.

The ideal circular polarisation is very hard to obtain, especially over a quite broad frequency band. According to the particular combination of the amplitude ratio and phase shift of the two orthogonal field components different polarisation states, more or less close to the pure circular one, are obtained. A measure of how the polarisation is close to the circular type is given by the axial ratio, plotted in Fig. 5 for this particular polariser.

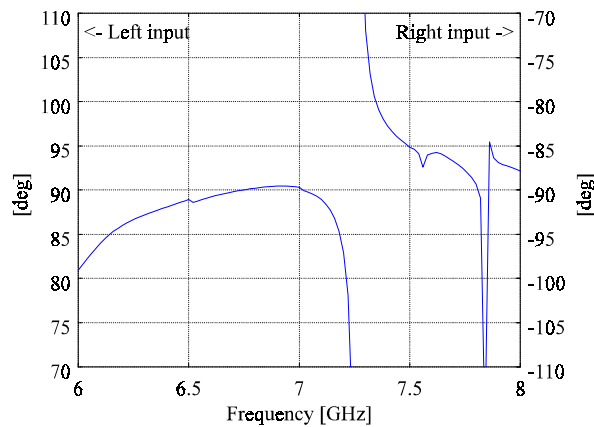


**Fig. 4:** Common port orthogonal polarisation phase shift (X-Y).

The axial ratio, usually expressed in dB, is the ratio of the  $90^\circ$  squared components of the field. The  $90^\circ$  squared components of a field are those components whose difference is  $90^\circ$  both in the space domain and in the time domain: that is the two components are orthogonal in space (like x and y versors) and a quarter wavelength phase shifted to each other.

It is possible to demonstrate that, given an arbitrary, sinusoidal, electromagnetic field, two such components always exist.

Because of the symmetry of the structure the axial ratio of the field in the common port is independent of the excitation port. The only difference is the rotation of the field: left hand or right hand respectively for left port or right port excitation.

From the plot in Fig. 5 we can notice that, also regarding polarisation aspects, the behaviour of the polariser is fairly dual-band (6-7.2 GHz and 7.4-7.7 GHz), the same conclusion as for matching considerations, previously done.

The axial ratio resonances (7.25 and 7.8 GHz) are originated by the bad return loss performance of the x directed component of the output port circular polarisation.

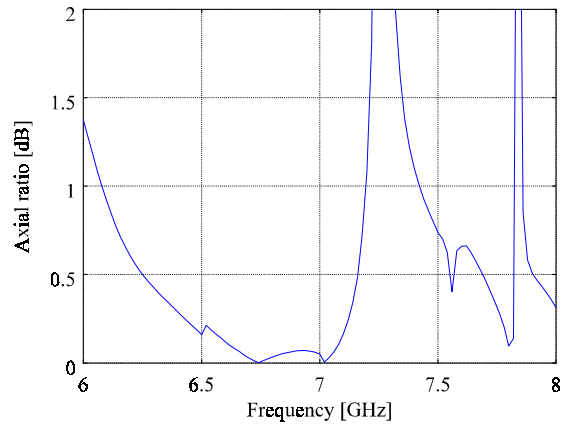


**Fig. 5:** Axial ratio of the common port field due to both left and right port excitation.

### 3 Polariser measurements:

A polariser prototype, based on the sketch in Fig. 1, has been realised in aluminium by direct machining (Fig. 6). The prototype is about 40 cm long with two WR137 input waveguides (at the top and the bottom on the left) and one output squared waveguide (on the right) referred to as the common output.

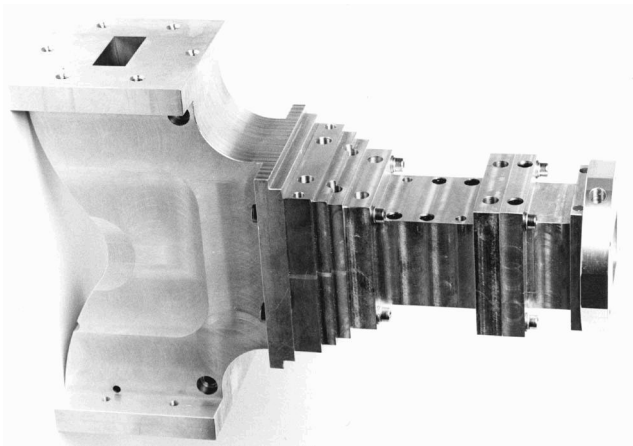


**Fig. 6:** Polariser prototype.

Three different test configurations are considered to measure the scattering parameters of the polariser prototype. The first one shown in Fig. 7 is formed by one two-port vector network analyser (VNA) as the main instrument, the device (polariser) under test (DUT), two N-type coaxial/WR137 calibrated transitions (CT) to connect the DUT to the VNA and finally one matched load (M) and one low loss, low VSWR (Voltage Standing Wave Ratio) WR137/squared transition (WST) to connect the common output (O) of the polariser to the CT.

With this set-up, four different sub-configurations can be used to measure both the reflection parameters at the common output port and the transmission between O and the two input ports, the right (R) and the left (L).

Let's consider first the configuration shown in Fig. 7. One port of the VA is connect, via the CT, to the R port of the polariser and the other is connect, via the CT and the WST exciting the linear x polarised field, to the O port. The L port is connect to the matched load. With this setup it is possible to measure the amplitude and phase of the x polarised field reflection at port O and its transmission to R. By interchanging the devices (M and CT)

connected to the input ports, it is possible to measure the amplitude and phase of the transmission parameter between O and L.

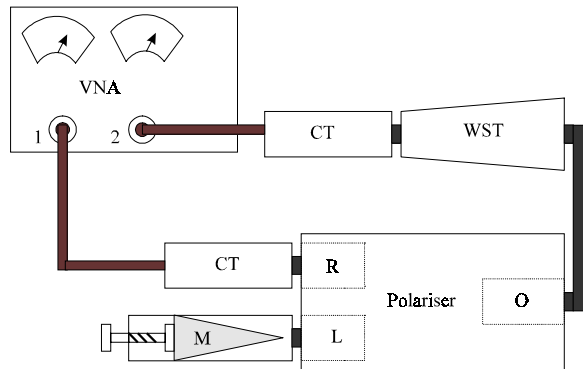


**Fig. 7:** Measurement set-up to obtain transmission parameters and reflection to the O port.

A  $90^\circ$  rotation of both the WST and the related CT around their axis allows the excitation of the y polarised field to the O port of the polariser. Repeating the above described procedure we can measure amplitudes and phases of the scattering parameters related to the linear y polarised field.

With a proper combination of the data obtained so far and by using the superposition principle we can have the following characterisation of the polariser:

- left circular polarisation reflection at O and transmission to L and R;
- right circular polarisation reflection at O and transmission to L and R.

By virtue of the reciprocity principle we can also obtain:

- L port transmission to left and right circular polarisation at O;
- R port transmission to right and left circular polarisation at O.

From the last two parameters we derive also the axial ratio.

It is important to notice that this set-up is unable to give the correct input reflection (L, R) and input cross-talk because of the presence of the WST in the output chain: this transition acts as a reactive load for one of the two polarisation components of the circular polarised excited field. For this reason one would have the ability to decompose the two different contributions at the input ports (L, R) in the measured reflection coming from the polariser (the one we would like to measure) and the WST (the unwanted or spurious one). This separation may be possible in principle, by using the time domain approach with the above set-up, but it's hard work in practice.

A WR137 to square transition as been designed and two identical parts has been realised. Firstly the transition has been characterised, by connecting the two parts together via the square end, leading to the results shown in Fig. 8.

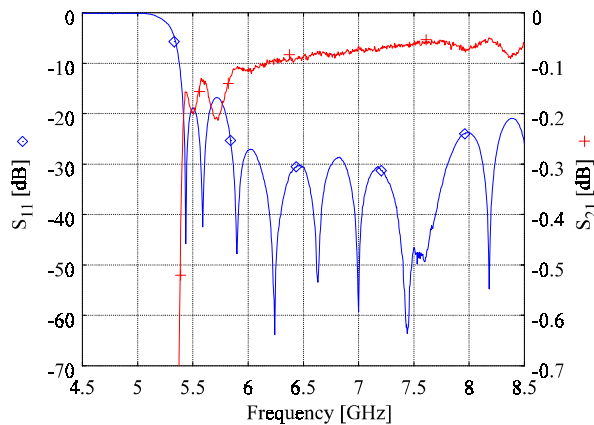


**Fig. 8:** Dual WR137 to square transition test: matching and losses.

Then the measurements of the polariser in the above described set-up have been started. From the measurements we have directly the output scattering parameters which are shown in Fig. 9 and compared with the simulations, highlighting very good agreement.

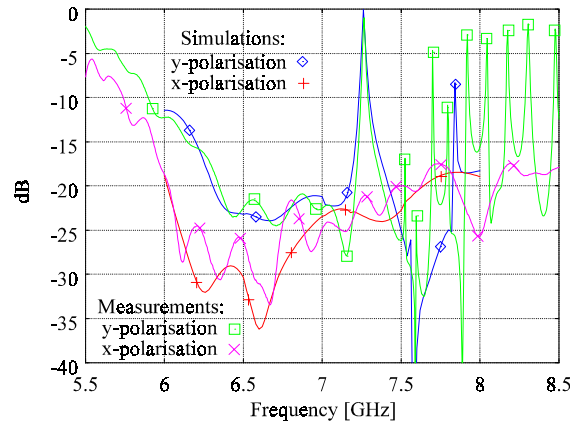


**Fig. 9:** Common port scattering parameters.

The multiple spurious resonances, related to the  $x$  polarisation measurements in the higher frequency band, are due to the coupling of the higher order modes (mainly the  $TE_{11}$  with 7.47 GHz cut-off frequency) with the WST part. These effects are not taken into account by the simulations we made and it has to be noticed that they only affect, in this higher band (7.47 – 8 GHz), this type of characterisation and not the polariser performances because of the absence of the WST in the operational environment. Further investigation for this aspect is needed.

The measured phase shift between the  $x$  and  $y$  polarised components of the output signal are given in Fig. 10, in the case of both L and R input port excitation.

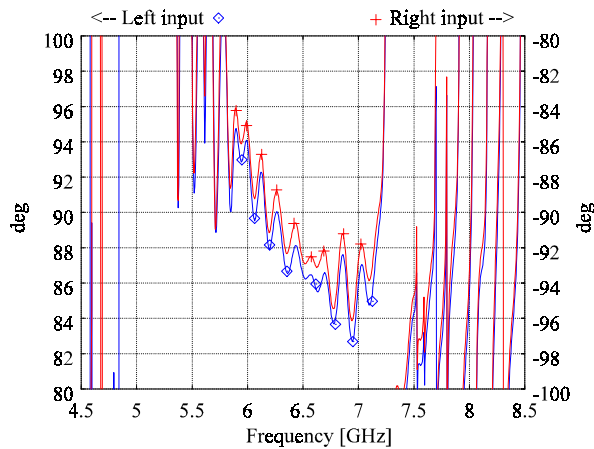


**Fig. 10:** Phase shift of the two orthogonal components ( $x$ - $y$ ) of the output circular polarisation .

The information related to the transmission parameters, both amplitude and phase, coming from the measurements have been used in the computation of the axial ratio, which is given in Fig. 11.

The curves quite agree with the simulations of Fig. 5 also if a small degradation has to be noticed in the 6 – 7.2 GHz band. For the spurious resonances in the upper part of the band, the same arguments discussed for the phase shift hold on concluding for the need of further investigation for more accurate characterisation.

To avoid the above described problems in the measurement of the scattering parameters at the input ports the set-up shown in Fig. 12 has been used because it's best suited to cancel spurious effects due to high order modes coupling in the common output region.

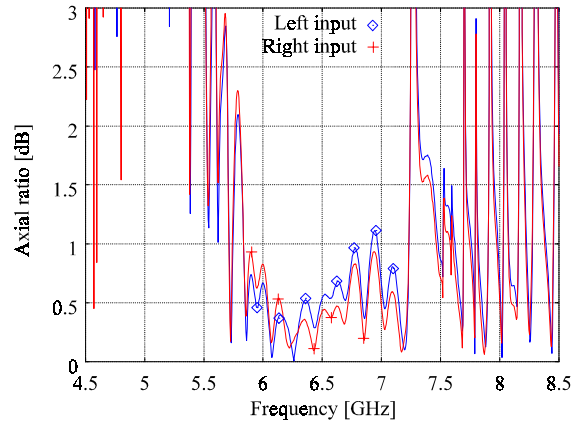


**Fig. 11:** Axial ratio for the left and right circular polarisations .

The two ports of the VNA are connected, via the CT, to the input ports (L,R) of the polariser. One not standard matched load, having a 28.4 mm<sup>2</sup> squared port, is directly connected to O. If available, the antenna employed in the actual operative environment may be used as a matched load, the higher the antenna return loss the better its behaviour as matched load. In this case the measure has to be made in an anechoic chamber or by putting some absorbing material in front of the antenna.

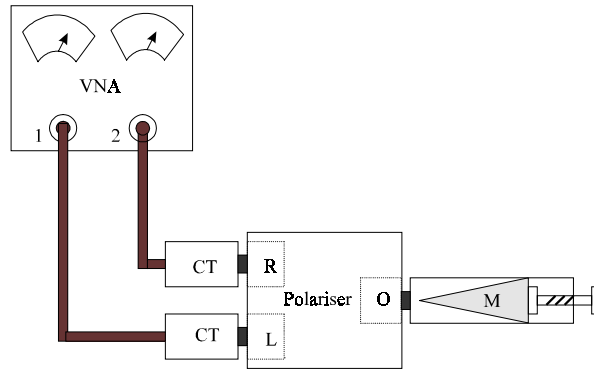


**Fig. 12:** Measurement set-up used for the reflection and cross-talk at the input ports (L,R).

The matched load used in the measurements is a waveguide ending with absorbing material. To test this matched load, it was connected via the WST and the CT to one port of the VNA and the results, given in terms of the reflection coefficient are shown in Fig. 13. We noticed that in the measured return loss there is also the contribution of the WST, which was not considered in the calibration chain, and so we can conclude that the matched load performances would be fairly better than those given in Fig. 13.

Although quite good, the matched load behaviour may have some influence on the reflection coefficient measurement of the polariser which is given in Fig. 14. This is particularly true at low levels (<25 dB) and partially accounts for the small differences between the measurements and the simulations. However they agree quite well as far as the shape and the precise prediction of the 7.25 GHz resonance are concerned. Another aspect that has influence on this is the presence of the dual E-plane bend in the prototype input ports, which was not considered in the model used for the simulations. Regarding instead the 7.8 GHz resonance which is present in the simulation plot but not in the measurements, this is caused by the squared to circular transition, considered in the simulation model but not used in the prototype characterisation.

Despite of those differences, the prototype behaviour is still good as regards the input match and the cross-talk. As expected, the use of the matched load in the common port leads to no spurious resonances in the upper part of the band for this kind of measurement. This fact can be interpreted as an encouraging sign to convince ourselves of the good behaviour of the polariser prototype also in the over-moded region (7.4 - 8 GHz).

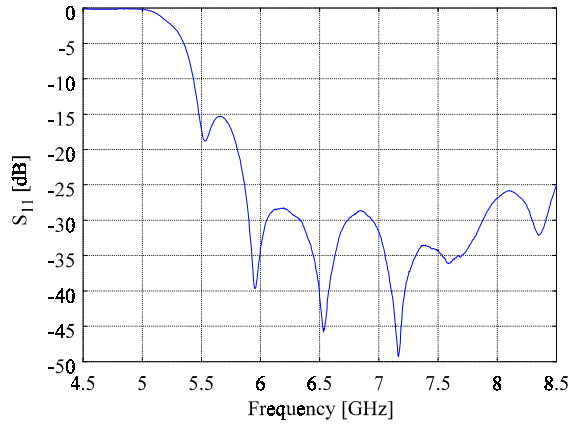


**Fig. 13:** Reflection coefficient of the absorbing material-ended waveguide used as matched load.

An alternative way to obtain the polariser input scattering parameters is to use the set-up shown in Fig.15. This configuration make use of two CT, two standard matched loads and two polariser prototype and may be most practical if more then one polariser prototype is intended to be fabricated.

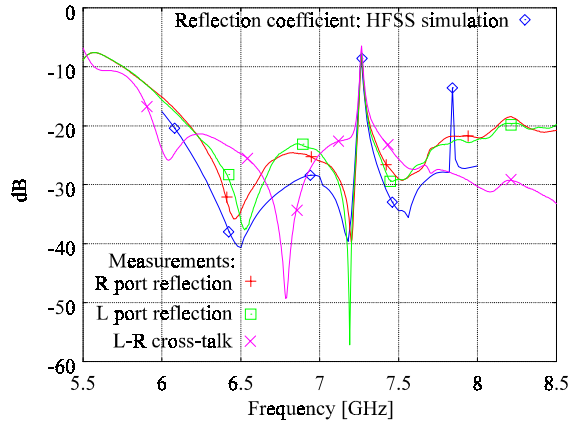


**Fig. 14:** Measurements of the 6 GHz septum polariser prototype: return loss and cross-talk.

The polarisers are joined through the O ports and the two couples of input ports are differently connected to the VA ports (via the CT) and to the matched loads, according to the parameters to be measured.

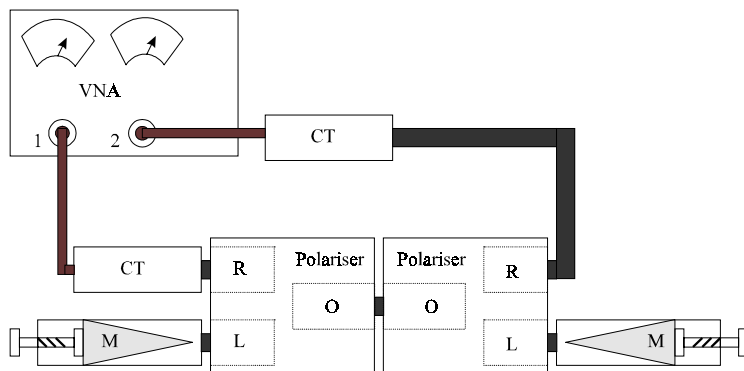


**Fig. 15:** Alternative set-up to obtain reflection and cross-talk at the input ports (L,R).

There is an issue related to the coupling of the O ports of the polariser that influence the measurements. This problem may be overcome by assuming that the two polarisers are equal (let's say their performances differ each

other less than the measure accuracy): with this assumption the contribution to the input parameter measurements coming from the O ports coupling may be extracted by calculations using direct measured data. A very accurate and efficient method to measure the losses of the polariser is to use the configuration shown in Fig. 16.

The network analyzer is connected to the input ports of the polariser and a conducting layer S (short circuit) is connected to the common output O. Because a metallic layer switches an incident left (right) hand circular polarised wave in a reflected right (left) hand circular polarised one, the idea is to associate the transmission between the rectangular ports to the losses (doubled) between each rectangular port and the common port. This method leads to some useful results only if each port of the polariser excites one of the two circular polarisation with low axial ratio. This is not a constriction in practice because in the operative band this assumption is valid. Moreover, the polarisation purity may be checked by measuring the return loss at each port: if this figure is high (greater than 20 dB) we can say that pure circular polarisation excitation condition (left or right hand according to the port under test) is satisfied.

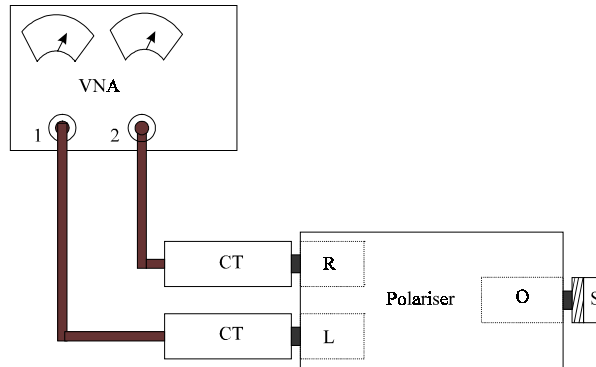


**Fig. 16:** Instrumental set up for loss measures.

The results are shown in Fig. 17. We can see a very low reflection coefficient in the 6 – 7.2 GHz band, confirming the already seen results (Fig. 11), that in this band almost pure circular polarisation is excited. From this measure we cannot state any figure about the axial ratio but we are quite confident that the opposite of the transmission coefficient (below 0.2 dB) is, with great accuracy, twice of the polariser insertion loss (between each rectangular port and the common port).

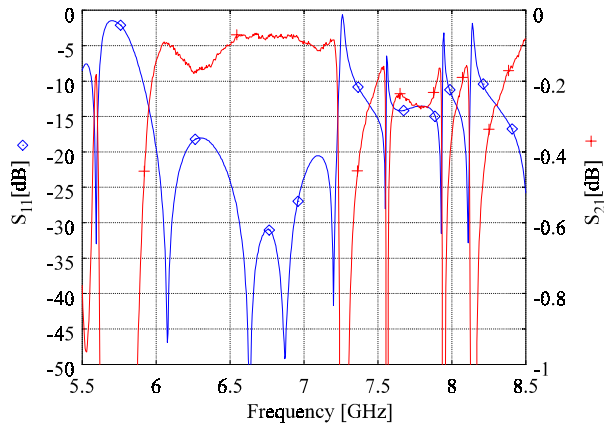


**Fig. 17:** Measurements of the 6 GHz septum polariser prototype: losses.

We can thus conclude that in the 6 – 7.2 GHz band the polariser losses are below 0.1 dB with a mean value of about 0.05 dB, which corresponds to a very low noise temperature of about 3.5 K at room temperature. In the upper 7.4 – 8.5 GHz band some resonances are present. We note that they are fewer and differently placed than the ones that appear in the Fig. 7 set-up measurements. This consideration lead us to enforce our conviction that in the upper band the resonances are related to the coupling between the output common port and the device

which, in the particular set-up, follows in the measurement chain (the WST in the previous case and the short in this latter case).

From  $S_{21}$  data it is possible to obtain the equivalent noise temperature of the polariser. A passive device characterised by a power loss  $A$ , shows an equivalent noise temperature given by  $T_n=(A-1)T_a$ , where  $T_a$  represents the room temperature.

By considering that  $S_{21}$  directly obtained by the measurements with the Fig. 16 set-up is the square (twice in dB, i.e. in logarithmic unit) of the actual transmission coefficient between one input port and the common output, due to the doubled path, this is also equal to the power gain of the polariser and therefore, by putting  $A= 1/S_{21}$  in the above formula, we obtain the equivalent noise temperature.

Taking as reference a room temperature  $T_a=300^\circ\text{K}$  we have the equivalent noise temperature plotted in Fig. 18.

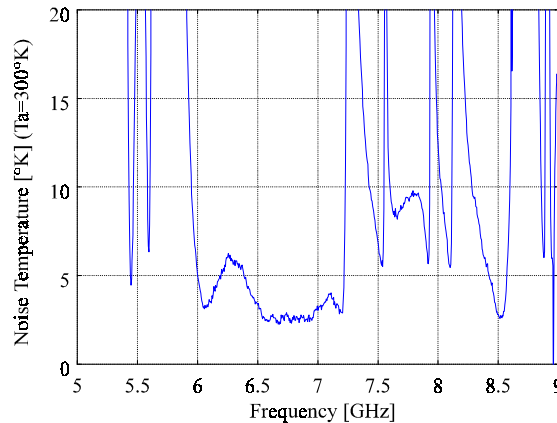


**Fig. 18:** Measurements of the 6 GHz septum polariser prototype: losses.

By using the first part of the three ones constituting a 6 GHz corrugated feed horn, further measurements have been carried out.

A first set-up is shown in Fig. 19, with the feed part (FIP) acting as a matched load attached to the common out of the polariser. In fact, as it can be noticed by the not very good cross talk curve in Fig. 20 the aperture effects have some influences and this is probably due to the small size of the feed part aperture. However these effects don't affect return loss because the aperture mismatch, due to the circular symmetry, splits a left-hand incident polarisation in a right-hand reflected one and vice versa. For this reason this set-up is valid and very accurate for reflection coefficient measurements. It has to be noticed that the experimental data agree quite well with simulation results.

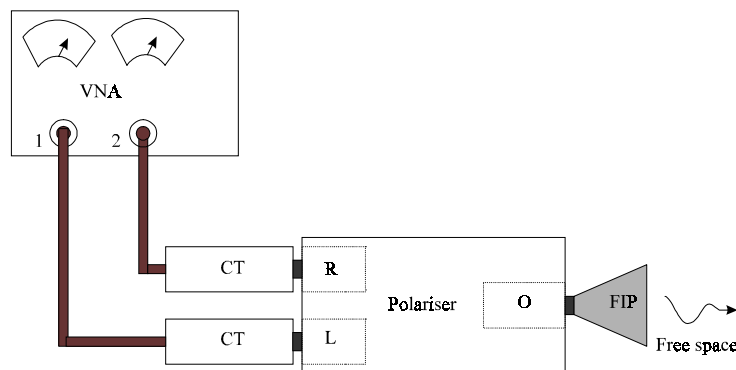


**Fig. 19:** Set-up for input reflection measurements.

An alternative way to the one shown in Fig. 16 for loss measurements is to use the configuration of Fig. 21, which has all the parts shown in of Fig. 19 with a conducting plate more placed on the horn aperture. This set-up has the advantage to take into account for the losses of the first part of the horn. However, because in this case, with respect to the configuration in Fig. 16, we have a longer distance (some wavelengths) between the polariser

septum and the short circuit, the resonant frequencies due to spurious mode coupling are different and densely placed.

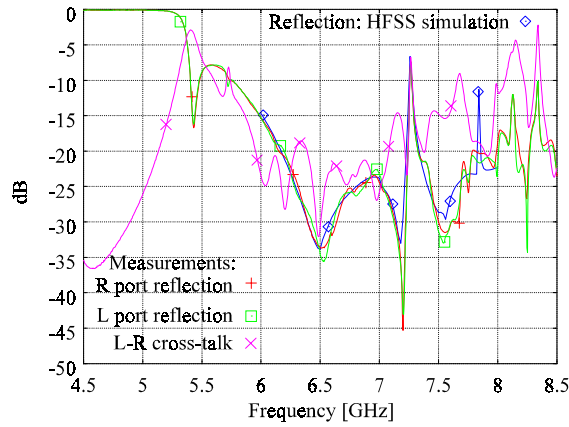


Fig. 20: Input reflection and cross talk.

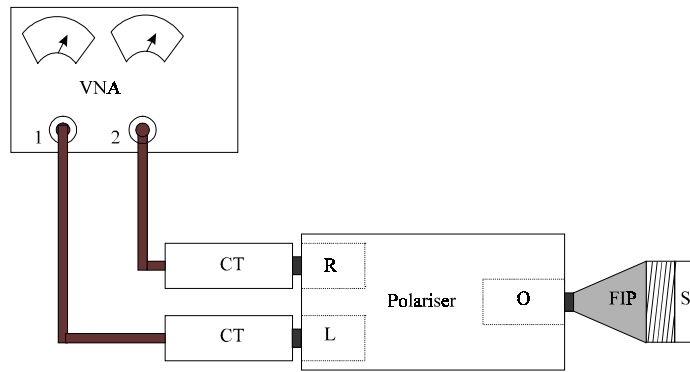


Fig. 21: Set-up for loss measurements.

Apart from this problems it has to be noticed in Fig. 22 a mean value of about 6°K for the noise temperature of this arrangement in the polariser band and by comparison with the plot of Fig. 18 we can evaluate the contribution of the feed initial part to the system noise temperature in about 2.5°K.

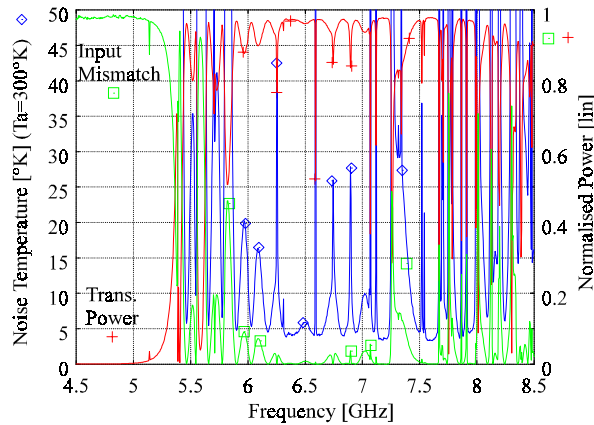


Fig. 21: Set-up for loss measurements.

This part of the feed, with respect to the remaining part, has a predominant effect on the feed losses, because it has a smaller section and so it is quite reasonable to estimate around 3°K the noise temperature of the entire feed.

## 4 Conclusions:

In this work the design of a 6 GHz septum polariser for a radio astronomy receiver has been addressed. The aim was to meet the requirements needed for the Noto and Arecibo radio telescopes.

After a brief theoretical introduction on the polariser behaviour, the design procedure has been presented.

A prototype has been built and measurement characterisation have been widely described, putting in evidence a very good behaviour in the 6 – 7.2 GHz frequency band.

While the design put in evidence an efficient behaviour of the polariser also in the 7.4 – 8 GHz frequency band, no accurate characterisation from a test point of view has been possible in that band and at present we cannot fully confirm, on the basis of the available measurements, the simulation results, also if we are quite confident on them.

## References:

- [1] J. Uher, J. Bornemann, U. Rosenberg, *Waveguide components for antenna feed systems : theory and cad*, Artech House, London, 1993.
- [2] R. Ihmels, U. Papziner, F. Arndt. "Field theory design of a corrugated septum OMT," in 1993 *IEEE MTT-S Int. Microwave Symp. Dig.*, pp. 909-912
- [3] P.P. Silvester, G. Pelosi, *Finite Elements for Wave Electromagnetics*, IEEE Press, New York, 1994.
- [4] R.Nesti, "Analisi di illuminatori rettangolari a step su piano di massa," Tesi di Laurea, Facoltà di Ingegneria, Università di Firenze, Giugno 1996.
- [5] H.Patzelt, F.Arndt, "Double-plane steps in rectangular waveguides and their application for transformers, irises, and filters," *Trans. Microwave Theory Tech.*, vol. MTT-30, no. 5, pp. 771-776, May 1992.